Identification of electrostatic and van der Waals interaction forces between a micrometer-size sphere and a flat substrate

B. Gady, D. Schleef, and R. Reifenberger
Purdue University, Department of Physics, West Lafayette, Indiana 47907

D. Rimai and L. P. DeMejo
Office Imaging Research and Technology Development, Eastman Kodak Company, Rochester, New York 14653-6402
(Received 15 August 1995; revised manuscript received 24 October 1995)

The interaction force gradient between a micron-size polystyrene sphere and an atomically flat highly oriented pyrolytic graphite substrate has been analyzed as a function of surface-to-surface separation distance z_0 using an oscillating cantilever technique. The interaction force gradient was found to have two contributions. For $z_0 \geqslant 30$ nm, an electrostatic force due to charges trapped on the polystyrene sphere dominates. For $z_0 \leqslant 30$ nm, a van der Waals interaction, characteristic of a sphere near a flat plane, is observed. Fits to the data are in good agreement with theoretical expectations and allow estimates of the surface charge density triboelectrically produced on the sphere's surface.

I. INTRODUCTION

The van der Waals force between two electrically neutral objects is a manifestation of a cooperative interaction between induced dipoles. A fundamental understanding of this force relies on a careful analysis of the fluctuations in the electric dipole fields due to polarizable atoms.[1,2] A characteristic signature of the van der Waals interaction between two polarizable atoms separated by distance z is a z^{-6} dependence for the interaction force. For the case of extended electrically neutral bodies, e.g., a sphere above a flat plane, a proper accounting of geometry must be included, resulting in an interaction force that varies with the sphere-substrate separation as z^{-2}. Since this effect is a macroscopic manifestation of cooperative behavior at the atomic length scale, measurements of the force and its dependence on material parameters are of continuing interest.[3,4]

The rapid development of the atomic force microscope (AFM) has produced techniques capable of measuring nanonewton forces acting on a sharp tip as it approaches a substrate. Under normal circumstances, it is generally assumed that the attractive force between the tip and substrate is governed by the van der Waals interaction. Quantitative measurements of the interaction force between a sharp tip and flat substrate are inherently difficult to interpret because the exact geometry of the tip is often not known. Various attempts to directly measure the spatial dependence of the attractive force between a tip and substrate have produced data that requires an action over a considerably greater range than expected if van der Waals forces are dominant. The appearance of this long-range force is often attributed to capillary effects due to unwanted contaminants. Recently, Burnham *et al.*[5] demonstrated that force measurements taken with a static cantilever approaching a surface can be fitted using a complicated electrostatic patch charge effect, providing an insight into the origin of the long-range force. Indeed, early attempts to study the van der Waals force between extended objects with dimensions greater than those considered here have emphasized the need to eliminate electrostatic forces.[6–8]

In what follows, we describe the results of experiments that have been designed to quantitatively investigate the transition between a long-range electrostatic and van der Waals force. We show that by attaching a micrometer-size polystyrene sphere to an AFM cantilever, ambiguities in the geometry of the two objects under study can be eliminated, resulting in data that can be quantitatively interpreted using standard models for interaction forces. We show that the interaction force gradient measured under moderate vacuum conditions can be quantitatively understood in terms of two contributions: for large sphere-substrate separations, a simple electrostatic interaction suffices to adequately explain the data, while for smaller separations, the data are well described by the van der Waals force appropriate for a sphere above a flat plane.

II. EXPERIMENTAL CONSIDERATIONS

The AFM used in these studies was a custom-built instrument that has been described elsewhere.[9] A freshly cleaved highly oriented pyrolytic graphite (HOPG) substrate was mounted onto a segmented PZT-5A piezoelectric tube and served as the atomically flat substrate. A second piezoelectric tube was used to hold a Si ultralever[10] and provided the oscillatory motion for the sphere attached to the cantilever. A polystyrene sphere was mounted on the edge of the cantilever using a microscopic drop of Norland Optical Cement No. 68 to the tip of the cantilever with the aid of an optical microscope system with an overall magnification of 750X. Experiments showed that this cement remained viscous for a sufficiently long time to accurately position the sphere on the cement with the aid of a micromanipulator. The particle was pressed into the cement to allow close contact of the particle with the cantilever. The cement was subsequently cured by exposure to UV light for approximately 10–15 minutes.[11] Detection of the cantilever displacement as a function of the sphere-substrate separation distance was done using a laser

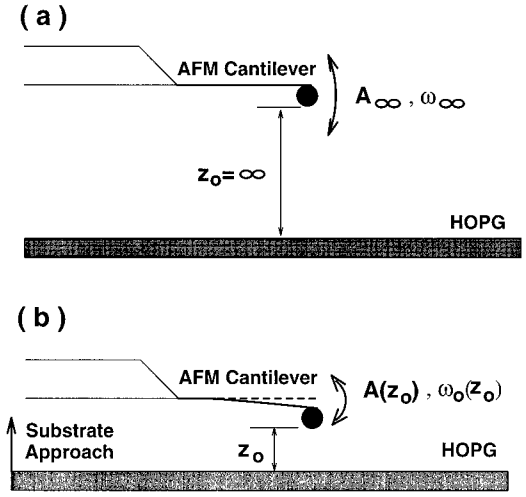

FIG. 1. Schematic diagram of the force gradient measurement. In (a), the cantilever is far from the substrate and the amplitude and frequency of oscillation are characterized by A_∞ and ω_∞. In (b), the sphere to substrate separation is decreased to a finite value z_0 and any interaction force between the sphere and substrate shifts the resonant frequency to $\omega_0(z_0)$ and reduces the amplitude of the cantilever's oscillation to $A(z_0)$.

deflection method and phase-sensitive detection.[12–14] A 68030 CPU based computer system, similar to that described previously,[15] controls the experiment. The spring constants of all cantilevers were independently calibrated using techniques discussed elsewhere.[16]

In order to minimize contamination due to water vapor and hydrocarbons on the surface, the entire AFM apparatus was mounted inside a small stainless steel chamber that could be evacuated to forepump pressures (~200 mTorr). Repeated pumping and backfilling with dry nitrogen gas provided a contamination-free environment for long-term storage of the sphere and substrate. In order to eliminate aerodynamic effects due to the oscillating cantilever, evacuation of the nitrogen gas was required prior to all data acquisition.

III. THEORETICAL CONSIDERATIONS

Noncontact (ac) force gradient data were obtained by measuring the amplitude of oscillation of the cantilever as a function of driving frequency for different sphere-substrate separations (see Fig. 1). Initial attempts to use an amplitude modulation technique,[17] in which the cantilever was driven at a frequency ω just off the resonance frequency ω_∞, were abandoned in favor of the frequency measurement technique,[18] which provides a direct method for calculating the interaction force gradient.

As discussed in Ref. 18, the equation of motion for a driven cantilever oscillating at a frequency ω at a position $z_{\rm eq}$ from the surface is

$$m\ddot{z}+\gamma\dot{z}-k(z-z_0)+F_{\rm inter}(z)=F_d\cos(\omega t), \qquad (1)$$

where m is the mass of the sphere, γ is a constant describing the damping of the cantilever, k is the measured spring constant of the cantilever ($\sim$ 2 N/m), $F_{\rm inter}$ is the interaction force of interest, and F_d is the driving force applied to the cantilever. A linear expansion can be made of the interaction force for the range of operation,

$$F_{\rm inter}=F_{\rm inter}(z_0)+\left(\frac{\partial F_{\rm inter}}{\partial z}\right)\Bigg|_{z_0}(z-z_0)+\cdots, \qquad (2)$$

giving an equation of motion of the form

$$m\ddot{z}+\gamma\dot{z}-k_{\rm eff}(z-z_0)=F_d\cos(\omega t)+\text{const} \qquad (3)$$

where

$$k_{\rm eff}=k-\left(\frac{\partial F_{\rm inter}}{\partial z}\right)\Bigg|_{z_0}. \qquad (4)$$

The oscillation amplitude is given by

$$A(\omega,z_0)=\frac{A_\infty}{\sqrt{[\omega^2-\omega_0(z_0)^2]^2+(\gamma\omega/m)^2}}, \qquad (5)$$

where the resonant frequency at the position z_0 is given by

$$\omega_0(z_0)=\omega_\infty\sqrt{1-\frac{1}{k}\left(\frac{\partial F_{\rm inter}}{\partial z}\right)}. \qquad (6)$$

Equation (6) provides a first-order approximation to the interaction force gradient in terms of $\omega_0(z_0)$, the measured resonance frequency as a function of position:

$$\frac{\partial F_{\rm inter}}{\partial z}=k\left[1-\left(\frac{\omega_0(z_0)}{\omega_\infty}\right)^2\right]. \qquad (7)$$

From this relation, a comparison of the inferred $\partial F_{\rm inter}/\partial z$ can be made to theoretical models.

IV. RESULTS

In this study, a lock-in amplifier is used to convert an oscillatory signal produced by the displacement of a laser beam reflected from the end of the oscillating cantilever to a dc signal, which is proportional to the amplitude of oscillation of the cantilever. This dc signal was monitored by the computer as the substrate was brought toward the cantilever in a controlled way. Knowledge of z_0, the equilibrium surface-to-surface separation between the sphere and substrate, is important when determining the power-law dependence of the interaction force gradient. If the spring constant of the ultralever is known, an estimate of the absolute separation distance can be made from the measured jump-to-contact distance. Measuring the jump to contact distance in this way served as an absolute calibration for our measurements, but precluded data for $z_0 \leqslant 5$ nm.

Representative data showing this shift in frequency and reduction in oscillation are shown in Fig. 2. Fitting Eq. (5) to this data, it is possible to accurately determine $\omega_0(z)$ and to calculate $k\{1-[\omega_0(z_0)/\omega_\infty]^2\}$. The logarithm of this quantity is plotted in Figs. 3(a) and 3(b) for 3 and 6 μm radius polystyrene spheres as a function of the sphere-substrate separation distance z_0.

Initially, attempts were made to fit the force gradient data using only a van der Waals force. All fits were found to have too short a range and were incapable of fitting the data at

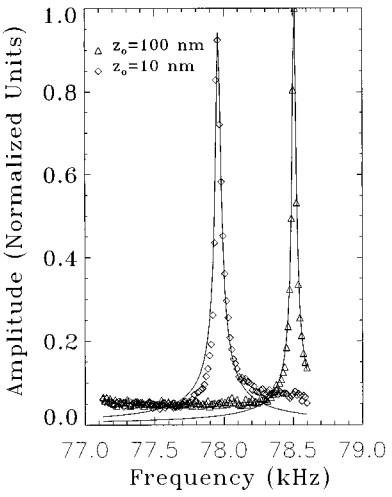

FIG. 2. The amplitude of the cantilever oscillation is given for two different values of z_0. The dashed line is a best fit to the data using Eq. (5).

large separation distances. As a consequence, other forces were examined, and ultimately a combination of forces were required to accurately describe the data. As a result of this analysis, it was concluded that for small separations ($z \leqslant 30$ nm), a van der Waals force gradient between a sphere and a flat plane, described by

$$\frac{\partial F_{\mathrm{vdW}}}{\partial z} = \frac{HR}{3z_0^3}, \tag{8}$$

fits the data quite well. Here, H is the Hamaker constant, R is the sphere radius, and z_0 is the surface-to-surface separation distance.

For larger separations, a long-range electrostatic force is required to understand the data. The origin of this electrostatic force is twofold. First, there are charges trapped around the perimeter of the polystyrene sphere. The surface charge density σ for these charges is $\sim 10^{-9}$ C/cm^2 as determined from independent Faraday cage measurements of the trapped charge on an ensemble of polystyrene spheres. A second contribution is the trapped charge that is likely to form on the bottom of the insulating polystyrene sphere when it "jumps to contact" with the substrate during the course of our measurements. It is interesting to further discuss the distribution of this charge, which is triboelectrically generated during the jump to contact of the sphere to the substrate.

When the sphere is in contact with the substrate, charge is free to flow in order to minimize the contact potential difference. In addition, the sphere deforms due to surface forces and touches the substrate over a finite area. The radius a_0 of this contact area can be estimated from the Johnson-Kendall-Roberts (JKR) theory, which analyzes the elastic deformation of a spherical object resting on a flat substrate.[19] This model has been successfully applied to studies of the deformation of micron-size spheres resting on substrates.[20,21] A well-known prediction of the JKR theory relates the contact radius of the contact at zero applied load a_0, to the elastic properties of the sphere by

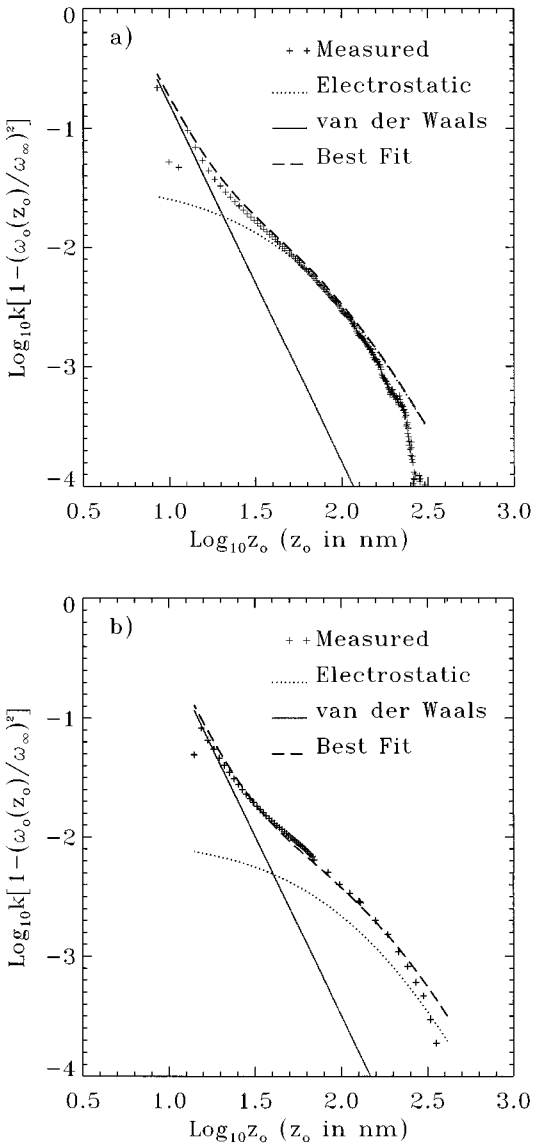

FIG. 3. Data measuring the force gradient of the interaction force between a polystyrene sphere and an atomically flat HOPG substrate. In (a), a plot of $\log_{10}(k\{1-[\omega_0(z_0)/\omega_\infty]^2\})$ vs $\log_{10} z_0$ (with z_0 in nm) for a 3-μm-radius sphere. The dashed line (see Table I) is the sum of the van der Waals and electrostatic contributions to the force gradient. In (b), a plot of $\log_{10}(k\{1-[\omega_0(z_0)/\omega_\infty]^2\})$ vs $\log_{10} z_0$ (with z_0 in nm) for a 6-μm-radius sphere. The dashed line (see Table II) is the sum of the van der Waals and electrostatic contributions to the force gradient.

$$a_0 = \left(\frac{6\pi R^2 W}{K}\right)^{1/3}, \tag{9}$$

where R is the sphere's radius, W is the work of adhesion given by

$$W = \gamma_{\mathrm{ps}} + \gamma_{\mathrm{HOPG}} - \gamma_{12}, \tag{10}$$

where $\gamma_{12} \simeq 2\sqrt{\gamma_{\mathrm{ps}}\,\gamma_{\mathrm{HOPG}}}$ and γ_{ps} and γ_{HOPG} are the surface-free energies of polystyrene and HOPG, respectively. The parameter K includes the elastic properties of the sphere and substrate and is given by

$$K=\frac{4}{3}\left(\frac{1-\nu_{ps}^2}{E_{ps}}+\frac{1-\nu_{HOPG}^2}{E_{HOPG}}\right)^{-1}. \quad (11)$$

Here, ν_{ps} and ν_{HOPG} are the Poisson ratios of polystyrene and HOPG, respectively, and E_{HOPG} and E_{ps} are the Young's moduli for HOPG and for polystyrene. Values for these quantities can be found in the literature.[22]

The electrostatic force between a grounded plane and a charge distributed over a sphere of radius R is discussed by Smythe.[23] For the case of a sphere of radius R at a potential V, whose center is located a distance $(z+R)$ from a grounded, conducting substrate, the force is given by

$$F_{el}=2\pi\epsilon_0 R^2 V^2\left[\frac{1}{2(z+R)^2}-\frac{8R(R+z)}{[4(R+z)^2-R^2]^2}+\cdots\right]. \quad (12)$$

The first term in this equation describes the force between a grounded conducting plane and a uniform charge distribution frozen in place on a sphere. The higher-order terms describe polarization effects that result when the sphere is moved closer to the plane. If the charges are trapped, as is the case here, only the first term is required. The potential of the sphere can be related to the charge Q on the sphere in the usual way, using the capacitance C of a sphere of radius R whose center is suspended a distance of $R+z$ above the plane

$$C=Q/V=4\pi\epsilon_0 R[1+r+\cdots], \quad (13)$$

where $r=R/2(R+z)$. Combining Eqs. (12) and (13) and taking the derivative provides an analytical expression for the force gradient due to electrostatics.

Attempts to fit the data using a uniform charge distribution trapped around the perimeter of the entire sphere produce a force gradient too small to fit the data. This result follows because, for the spheres used in this study, $R \gg z_0$. This led us to consider triboelectrically produced charges trapped at the bottom of the sphere. In this regard, it was assumed that upon jump to contact of the sphere to the substrate, a region of the sphere of radius $\sim a_0$ [see Eq. (9)] makes contact with the substrate and becomes locally charged. Upon withdrawal, this charge resides in a spherical region of size R_{eff} where $R_{eff} \simeq a_0$. This charge remains trapped at the bottom of the sphere in the vicinity of the contact region. This situation is illustrated schematically in Fig. 4. Under these circumstances, the electrostatic force is determined by modeling the trapped charge as a spherically symmetric distribution of radius $R_{eff} \simeq a_0$.

The determination of the best parameters to fit the data is facilitated by the fact that Eq. (8) is dominant for small sphere-substrate separations, while Eq. (12) is important for larger values of z. We find no need to include retardation effects in this discussion because optical absorption measurements on polystyrene show a strong absorption around 300 nm. This wavelength defines the transition region between retarded and nonretarded van der Waals interactions; however, the electrostatic interaction dominates in this transitional region.

The fits to the experimental data are shown by the dashed lines in Figs. 3(a) and 3(b). R_{eff} and H were adjusted until reasonable agreement with the data was obtained. The parameters determined in this way are given in Tables I and II.

TABLE I. 3-μm-radius sphere.

Parameters	Expected values	Fitted values
H	1.1 eV[a]	1.0 eV
R	3.0 μm	3.0 μm
R_{eff}	160 nm[b]	80 nm
Q		400 e^-
σ	$\sim 10^{-9} C/cm^2$ [c]	8×10^{-8} C/cm^2

[a]Interactions between polystyrene and graphite (Ref. 24).
[b]Contact radius based on JKR model.
[c]Faraday cage measurement of charge on an ensemble of polystyrene spheres (Ref. 25).

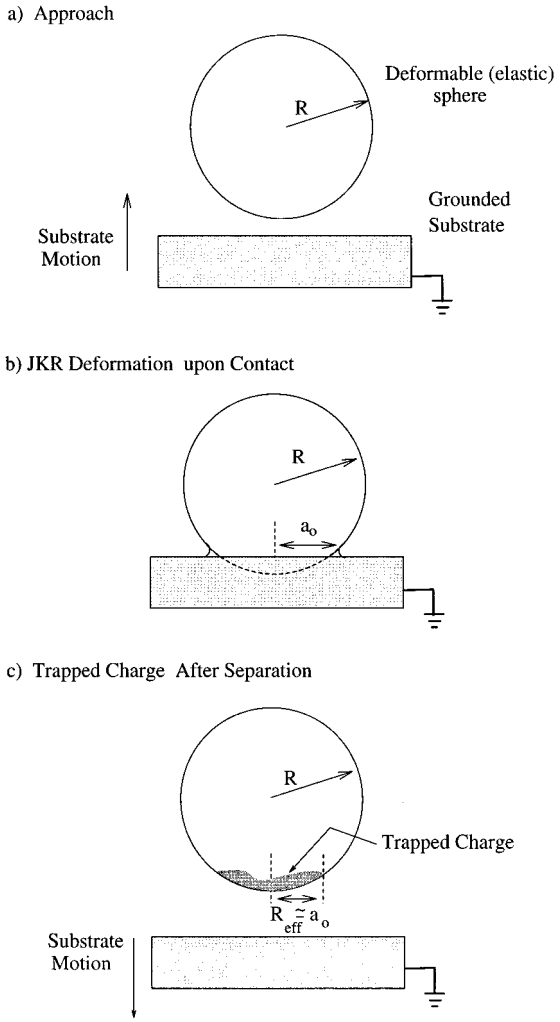

FIG. 4. The relevant parameters to describe triboelectric charging of the polystyrene sphere upon contact and removal from an atomically flat HOPG substrate. In (a), a sphere of radius R approaches the HOPG substrate. Upon contact (b), the sphere deforms due to surface forces between the sphere and substrate, which cause a contact area to form with radius a_0. While in contact, charge transfer between the grounded substrate and the sphere takes place. After separation, the excess charge remains localized at the bottom of the sphere over a region with radius $R_{eff} \simeq a_0$.

TABLE II. 6-μm-radius sphere.

Parameters	Expected values	Fitted values
H	1.1 eV[a]	1.0 eV
R	5.5 μm	6.0 μm
R_{eff}	270 nm[b]	140 nm
Q		700 e^-
σ	$\sim 10^{-9} C/\text{cm}^2$ [c]	5×10^{-8} C/cm^2

[a]Interactions between polystyrene and graphite (Ref. 24).
[b]Contact radius based on JKR model.
[c]Faraday cage measurement of charge on an ensemble of polystyrene spheres (Ref. 25).

Based on the models used, there is reasonable agreement between expected and fitted values for each parameter. The value used for the Hamaker coefficient for each sphere agrees closely with the expected value determined using the modified Lifshitz model for the van der Waals interaction between polystyrene and graphite.[24] The radius of each sphere as measured using a 750X optical microscope is consistent with the values required to fit the data for each sphere. A factor of 2 discrepancy exists between fitted values for the effective radius of charge transfer and estimates based on the JKR model of adhesion. At this time, this seems acceptable since a detailed model for charge transfer has not yet been developed for this system. In addition, the JKR theory does not account for such factors as surface roughness, which is probably nonnegligible for the polystyrene spheres used here. The discrepancies between expected and fitted charge denisties, σ, are thought to occur because the Faraday cage measurement values are an average over a large ensemble of polystyrene spheres. These Faraday values are, nonetheless, useful because they provide confirmation that the fitted charge densities are not grossly in error.

V. SUMMARY

Using an amplitude modulation technique, a method has been described that allows an accurate analysis of the interaction force gradient between individual micron-size polystyrene spheres and a flat HOPG substrate. For surface-to-surface separations $z_0 \geqslant 30$ nm, a long-range electrostatic force is required to understand the data. Fits to the data indicate that a charge of $\sim$500 electrons are distributed over a region at the bottom of the sphere with an effective radius of $\sim$100 nm. The origin of this trapped charge is thought to be related to triboelectric charging that occurs when the sphere jumps to contact with the substrate during the course of these measurements. The localized charge is larger than results from Faraday cage measurements, which are an average over a large number of particles. While the results are not directly comparable, they do indicate the magnitude of charge that can be acquired. The effective radius over which this charge is distributed is consistent with expectations based on the radius of contact of each sphere with the substrate using the JKR elastic deformation model. The discrepancies between the expected and fitted values for the effective radius of each sphere might be explained by surface roughness. The force at sphere-substrate separations $z_0 \leqslant 30$ nm is well described by a van der Waals interaction. Estimates of the Hamaker coefficient required to fit the data are in good agreement with values published previously. No data are available for surface-to-surface separations less than $\sim$5 nm due to the jump to contact of the sphere to the substrate.

Using the techniques discussed above, a systematic study of the interaction force gradient between a wide variety of different micron-size objects and flat substrates now seems feasible. Utilizing these techniques, a better understanding of adhesion and nanoindentation effects in a wide variety of materials will result.

ACKNOWLEDGMENTS

The authors would like to thank D. Schaefer and D. Krause for their helpful discussions during the initial stages of this work. This work was partially funded by the Office Imaging Division of Eastman Kodak Company.

[1] D. Langbein, in *Theory of van der Waal's Attraction*, Springer Tracts in Modern Physics Vol. 72 (Springer-Verlag, New York, 1972).
[2] L. Spruch, Phys. Today **39** (11), 37 (1986).
[3] W. Arnold, S. Hunklinger, and K. Dransfeld, Phys. Rev. B **19**, 6049 (1979).
[4] V. Sandoghdar, C. I. Sukenik, E. A. Hinds, and S. Haroche, Phys. Rev. Lett. **68**, 3432 (1992).
[5] N. A. Burnham, R. J. Colton, and H. M. Pollock, Phys. Rev. Lett. **69**, 144 (1992).
[6] B. V. Derjaguin, I. I. Abrikosova, and E. M. Lifshitz, Q. Rev. Chem. Soc. (London) **10**, 295 (1956).
[7] W. Black, J. G. V. De Jongh, T. G. Overbeek, and M. J. Sparnaay, Trans. Faraday Soc. **56**, 1597 (1960).
[8] S. Hunklinger, H. Geisselmann, and W. Arnold, Rev. Sci. Instrum. **43**, 584 (1972).
[9] D. M. Schaefer, A. Ramachandra, R. P. Andres, and R. Reifenberger, Z. Phys. D **26**, S249 (1993).
[10] Available from Park Scientific Instruments, Sunnyvale, CA, 94089.
[11] D. M. Schaefer, M. Carpenter, B. Gady, R. Reifenberger, L. P. DeMejo, and D. S. Rimai, J. Adhes. Sci. Technol. **9**, 1049 (1995).
[12] G. Meyer and N. M. Amer, Appl. Phys. Lett. **53**, 1045 (1988).
[13] G. Meyer and N. M. Amer, Appl. Phys. Lett. **53**, 2400 (1988).
[14] S. Alexander, L. Hellemans, O. Marti, J. Schneir, V. Elings, P. K. Hansma, M. Longmire, and J. Gurley, J. Appl. Phys. **65**, 164 (1989).
[15] R. Piner and R. Reifenberger, Rev. Sci. Instrum. **60**, 3123 (1989).
[16] J. P. Cleveland, S. Manne, D. Bocek, and P. K. Hansma, Rev. Sci. Instrum. **64**, 403 (1993).

[17] Y. Martin, C. C. Williams, and H. K. Wickramasinghem, J. Appl. Phys. **61**, 4723 (1987).
[18] W. A. Ducker, R. F. Cook, and D. R. Clarke, J. Appl. Phys. **67**, 4045 (1990).
[19] K. L. Johnson, K. Kendall, and A. D. Roberts, Proc. R. Soc. London Ser. A **324**, 301 (1971).
[20] D. S. Rimai, L. P. DeMejo, and R. C. Bowen, J. Appl. Phys. **68**, 6234 (1990).
[21] D. S. Rimai, L. P. DeMejo, W. B. Vreeland, R. C. Bowen, S. R . Gaboury, and M. W. Urban, J. Appl. Phys. **71**, 2253 (1992).
[22] D. W. van Krevelen, *Properties of Polymers* (Elsevier, New York, 1976).
[23] W. R. Smythe, *Static and Dynamic Electricity* (McGraw-Hill, New York, 1939).
[24] H. Krupp, Adv. Colloid Interface Sci. **3**, 137 (1972).
[25] D. Rimai (private communication).